Characterization of inorganic phosphate transport in the triple-negative breast cancer cell line, MDA-MB-231

Thais Russo-Abrahão[1,2☯]**, Marco Antônio Lacerda-Abreu**[1,2☯]**, Tainá Gomes**[1]**, Daniela Cosentino-Gomes**[1,2]**, Ayra Diandra Carvalho-de-Araújo**[1,2]**, Mariana Figueiredo Rodrigues**[1]**, Ana Carolina Leal de Oliveira**[1]**, Franklin David Rumjanek**[1]**, Robson de Queiroz Monteiro**[1]**, José Roberto Meyer-Fernandes**[1,2]*

1 Instituto de Bioquímica Médica Leopoldo De Meis, Centro de Ciências da Saúde, Universidade Federal do Rio de Janeiro, Rio de Janeiro, RJ, Brazil, 2 Instituto Nacional de Ciência e Tecnologia em Biologia Estrutural e Bioimagem, Rio de Janeiro, RJ, Brazil

☯ These authors contributed equally to this work.
* meyer@bioqmed.ufrj.br

Abstract

Background

Recent studies demonstrate that interstitial inorganic phosphate is significantly elevated in the breast cancer microenvironment as compared to normal tissue. In addition it has been shown that breast cancer cells express high levels of the NaP$_i$-IIb carrier (SLC34A2), suggesting that this carrier may play a role in breast cancer progression. However, the biochemical behavior of inorganic phosphate (P_i) transporter in this cancer type remains elusive.

Methods

In this work, we characterize the kinetic parameters of Pi transport in the aggressive human breast cancer cell line, MDA-MB-231, and correlated P_i transport with cell migration and adhesion.

Results

We determined the influence of sodium concentration, pH, metabolic inhibitors, as well as the affinity for inorganic phosphate in P_i transport. We observed that the inorganic phosphate is dependent on sodium transport ($K_{0,5}$ value = 21.98 mM for NaCl). Furthermore, the transport is modulated by different pH values and increasing concentrations of P_i, following the Michaelis-Menten kinetics ($K_{0,5}$ = 0.08 mM P_i). PFA, monensin, furosemide and ouabain inhibited P_i transport, cell migration and adhesion.

Conclusions

Taken together, these results showed that the uptake of P_i in MDA-MB-231 cells is modulated by sodium and by regulatory mechanisms of intracellular sodium gradient.

Abbreviations: DMSO, dimethyl sulfoxide; EDTA, ethylenediamine tetraacetic acid; FBS, foetal bovine serum; HEPES, 4-(2-hydroxyethyl)-1-piperazineethanesulfonic acid, PFA, phosphonoformic acid.

General Significance: Pi transport might be regarded as a potential target for therapy against tumor progression.

Introduction

Phosphorus is an essential element found in all forms of life. In mammals, it is obtained from the diet in the anionic form of Pi (H_2PO^{-4} or HPO^{-4}) through absorption in the small intestine [1]. Inorganic phosphate (Pi) plays a critical role in several cellular processes such as energy metabolism, either in the form of ATP by the energy transfer mechanism, or in its free form as substrates for intermediates of metabolic pathways. As a constituent of ATP, Pi also participates in the mechanisms of phosphorylation and dephosphorylation of intermediates of cellular signaling events. Pi is a fundamental component of phospholipids and nucleotides of DNA and RNA [2]. To satisfy the phosphorus requirements of a healthy mammal, the extracellular Pi is maintained under a relatively narrow range of concentration, between 0.8 and 1.5 mM [1]. Under physiological conditions, Pi is an anionic molecule and, therefore, its diffusion through the membrane lipid bilayer is hindered, requiring thus a protein transport system for translocation from the extracellular to the intracellular medium [3]. In mammals, several inorganic phosphate transporters have been described and can be classified into three different protein families denoted NaPi-I, NaPi-II and NaPi-III. NaPi-I (NPTI) is predominantly expressed in the border membrane of the proximal tubular brush, and functions as an intrinsic Pi transport modulator, [4]. NaPi-II (SLC34) is a sodium-dependent phosphate transporter that carries the phosphate in its monovalent form. It is further classified in the following subfamilies: NaPi-IIa (SLC34A1), NaPi-IIb (SLC34A2), and NaPi-IIc (SLC34A3); NaPi-IIb is found in breast cells [1,5,6,7,8]. The type III, NaPi-III (SLC20) transporters family, comprises proteins responsible for a sodium-dependent phosphate transport in its monovalent form. NaPi-III is divided in two subfamilies: PiT-1 (SLC20A1) and PiT-2 (SLC20A2) [1,4,5,6].

Genome–wide analysis strongly suggests that mutations affect both branches of the regulatory pathways that contribute, simultaneously or not, towards tumorigenesis, namely oncogenes and tumor suppressor genes. These may determine the gain of function of genes dictating growth control and cell survival and inactivate genes that in normal cells promote apoptosis [9]. Given the high degree of interactivity of the network involving cellular signaling pathways and the accumulating evidence assigning to metabolic enzymes the dual role of transcription factors [10], it is not surprising that the cell proliferation and invasiveness typical of cancer cells are intimately connected to metabolic reprogramming and hence a distinct bioenergetic phenotype [11]. The "growth rate hypothesis" was described in cancer cells and it was demonstrated that tumors have elevated phosphorus demands associated with protein synthesis and accelerated proliferation [12]. According to this theory, high phosphorus is required for the rapid growth of tumor, thus having a role in tumorigenesis and tumor progression. Recently, it was observed that the Pi concentration in the tumor microenvironment of breast tumors is significantly elevated as compared to normal mammary glands. In addition, authors documented increased Pi concentrations in highly metastatic tumor xenografts as compared to non-metastatic tumors [13].

There are three important receptors involved with classification of breast cancer: the receptors for the estrogen (ER) and progesterone (PR) hormones or epidermal growth factor receptors (HER-2) [14,15]. According to the classification based on the expression patterns of receptors in breast cancer, there are four molecular subtypes were found: luminal A, luminal B, HER2 and triple-negative overexpression [16]. The MDA-MB-231 cell line (classified in the

triple-negative molecular subtype) is a cellular model with a high metastatic capacity and, therefore, is considered a more aggressive strain compared to MCF-7 (ER+, PR+ and HER is classified as a tumorigenic, but non-metastatic cell line) [17,18].

MDA-MB-231 cells exhibit increased migratory capacity upon increasing Pi concentrations in the growth medium. There are two solute carrier families of Pi transport in mammals: SLC20 and SLC34 and both protein families transport Pi using the electrochemical gradient for Na+ [19]. It has been previously described that NaPi-IIb (SLC34A2) is up-regulated in ovarian carcinomas and benign tumors compared to normal ovary tissues [20]. Another study showed that the upregulated expression of SLC34A2 in hepatocellular carcinoma cell lines, and the knockdown of this Pi transporter decrease cell proliferation, migration and invasion as well as the epithelial–mesenchymal transition [21]. In lung cancer cells, SLC34A2 was also necessary for proliferation and tumorigenesis [22]. Overexpression of the NaPi-IIb transporter has been described in breast cancer tumors as opposed to normal tissues and has been proposed as a novel diagnostic marker and a therapeutic target [23]. Thus, the aim of this study was to characterize the Pi transport kinetics in the MDA-MB-231 breast cancer cell line by investigating whether such biochemical features may suggest interference tactics using inhibitors that could impact upon migration and invasive capacity.

Materials and methods

Materials

Reagents were bought from E. Merck (Darmstadt, Germany) and Sigma Chemical Co. (St. Louis, MO, USA). Radioactive inorganic phosphate ($^{32}P_i$) used was from Instituto de Pesquisas Energéticas e Nucleares (IPEN). In this work, we used distilled water through a Milli-Q system of resins to prepare all solutions (Millipore Corp., Bedford, MA, USA).

Cell culture

MDA-MB-231, T47D and MCF-7 cells were grown at 37˚C in Iscoves Modified Dulbeco's Medium (IMDM—LCG Biotechnology, Brazil) supplemented with sodium bicarbonate, 10% of foetal bovine serum (FBS) (Cripion Biotechnology, Brazil), 100 U/mL penicillin and streptomycin (Thermo Fisher, Brazil). 67NR and 4T1 cell lines, which originated from a spontaneous mammary carcinoma arising in a BALB/c mouse [24], were purchased from Karmanos Cancer Institute (Detroit, MI, USA). Cells were maintained in high glucose Dulbecco's modified Eagle medium (DMEM), supplemented with L-GlutaMax, 10 mM sodium carbonate, Hepes Buffer and 10% FBS and maintained at 37˚C in a humidified atmosphere of 5% CO_2. For the experiments, cells were harvested from the culture medium, washed two times with buffer comprising of 116 mM NaCl, 5.4 mM KCl, 5.5 mM glucose, 0.8 mM $MgCl_2$ and 50 mM HEPES (pH 7.2). Hank's EDTA solution was used to isolated cells from dishes. Cell number was estimated by counting in a Neubauer chamber. The protein concentration was measured with the Bradford methodology [25].

Pi transport assay in MDA-MB-231

Living MDA-MB-231 cells (10^4 cells) were incubated at 37˚C for 1 hour in a reaction mixture (0.5 mL) containing 116 mM NaCl or choline chloride, 5.4 mM KCl, 5.5 mM glucose, 50 mM HEPES (pH 7.2), 0.8 mM $MgCl_2$, 0.1 mM KH_2PO_4 and 2.5 µCi/nmol $^{32}P_i$ [26]. The reaction was stopped with 0.5 ml of an ice-cold PBS buffer (pH 7.2). Cells were washed with the same cold buffer at 4˚C and disrupted with 0.25 mL Hank's solution (5.37 mM KCl, 0.44 mM KH_2PO_4, 136.8 mM NaCl, 0.33 mM NaH_2PO_4, 5.03 mM D-glucose, 4.16 mM sodium

bicarbonate, 6.35 mM EDTA, pH 7.2) and 0.25 ml 0.1% SDS. These lysed cells with the internalized Pi were moved to a filter paper and, then, to a scintillation liquid. Blank values of uptake were obtained as previously described [26].

It was used 0 to 0.5 mM of Pi to measure the substrate affinity ($K_{0.5}$) and maximum rate (V_{max}) of the P_i transporter. Bafilomycin A_1 (100 nM), a vacuolar ATPase inhibitor, and valinomycin (100 μM), the K^+ ionophore, were also tested. Monensin (100 μM), a Na^+ ionophore, furosemide (1 mM), a Na^+-ATPase inhibitor and ouabain (1 mM), a Na^+,K^+-inhibitor, were tested. The H^+,K^+-ATPase inhibitor, SCH28080 (100 μM) and the P_i transport inhibitor, phosphonoformic acid (PFA—5 mM) were also tested. Vehicles: DMSO 1% (bafilomycin A_1, valinomycin, furosemide and SCH28080), ethanol 1% (monensin), water (ouabain and PFA); controls were performed using these vehicles. At 1% of these vehicles, the values for $^{32}P_i$ uptake obtained were the same obtained with water. The viability of MDA-MB-231 was verified according to the manufacturer's instructions of CellTiter 96® AQueous One Solution Cell Proliferation Assay (MTS) (Promega, EUA).

Real-time PCR analysis

Total RNA was purified from MDA-MB-231 cells using TRIzol Reagent (Invitrogen, Thermo Fisher Scientific, Massachusetts, USA) as described by manufacturer's manual. After treatment of RNA with DNase I, a first-strand synthesis kit (Invitrogen) was used to generate full-length cDNA from 1 μg of total RNA. qPCR was carried in StepONE Plus Real Time PCR System (Applied Biosystems, Massachusetts, USA), using a FastStart Master SYBR Green I Kit (from Roche, Mannheim, Germany). The primers for amplification are shown in Table 1. Gene expression data were normalized to an endogenous reference β-actin (ACTB) as previously described [27], and according to the manufacturer's instructions.

Migration assay

Tumor cell migration was assayed in a 48-well Boyden chamber (Neuro Probe Microchemotaxis System, Gaithersburg, MD) using 12-μm polycarbonate filters, as previously described [28]. 28 μl of IMDM containing 2.5% FBS was added at the bottom of the chamber as the chemoattractant. At the upper part, 5 x 10^4 cells/well, pretreated with ouabain, furosemide, monensin or phosphonoformic acid (PFA) for 1h, was added in 50 μL of medium in the absence of FBS. Controls were performed by pretreating the cells, for 1 h, in the specific drug diluents: 1% DMSO or 1% ethanol in 50 μL of medium in the absence of FBS., After migration for 1.5h, filters were removed from the chambers, fixed and stained with Panoptic kit (Interlab, São Paulo, Brazil). Tumor cells that had migrated through the membrane were counted in a LX400 light microscopy under a 100 x objective (Labomed Inc, Los Angeles, CA) on at least five random fields. The results are representative of three independent experiments performed in triplicate.

Table 1. Primers sequences.

Sequence name	Sense primer (5'– 3')	Antisense primer (5'– 3')
NaPi 1	CGTATGTCTTCTCTGGTTCGTTCTG	CGTAAAACTACCAGTGGAAATAGCCC
NaPi-IIa	GTGGCCTCCTTCAACATCCAT	CTGTAAGGAGTCTGGGTGGC
NaPi-IIb	CCCAGCTTATAGTGGAGAGCTTC	GCACCAAATCTTGACAAGACTCTTG
NaPi-IIc	GAATTTCAGAGGGCTTTCAGCG	GAGTCCAACTGCACGATGAGG
ACTB	TGACGTGGACATCCGCAAAG	CTGGAAGGTGGACAGCGAGG

Adhesion assay

96-well tissue culture plates were performed pre-coated with 32 µg/mL ECM gel (from mouse sarcoma) diluted in phosphate buffered saline (PBS), 100 µL per well for overnight in 4˚C and non-specific binding sites in the wells were blocked with 1 mg/mL BSA diluted in PBS for 2 h at room temperature. Cells grown at 80% confluency in IMDM with 10% FBS were pretreated with the phosphate transport inhibitors for 1h, then the cells were trypsinized, suspended in serum-free medium at the concentration of 2×10^4 cells/mL and applied 100 µL for each well incubated under routine condition as above for 3h. After incubation, non-adherent cells were removed by carefully washing twice with PBS, fixed with 3% paraformaldehyde for 10 min. Cleaned with PBS two times, stained with 100 µL 0.5% crystal violet for 5 min, washed two times and lysed with 100 µL ethanol of 1% acetic acid solution read at A570. Results were expressed 100% as control [29].

Statistical analysis

All experiments were performed, at least, three times in triplicate. The experiments were represented with values of mean ± SE. We used nonlinear regression analysis of the data to the Michaelis–Menten equation ($K_{0.5}$ and V_{max} values). Significant differences: $p < 0.05$. Statistical analyses were performed using Prism 6.0 software (GraphPad Software, San Diego, USA).

Results

Pi transport in different lineages of breast cancer cells

In an initial approach, we assayed the Pi transport in three different human breast cancer cell lines. When we compared them, the most aggressive, MDA-MB-231, had the higher P_i transport activity (Fig 1A). In addition, we employed two isogenic murine breast cancer cells: 67NR, is a low-aggressive, nonmetastatic, cell line and 4T1, is a highly aggressive, metastatic, cell line [24]. As seen in the human cell lines, 4T1 cells presented higher $^{32}P_i$ transport than 67NR (Fig 1B). Based on these initial results, we opted to concentrate our study specifically on the MDA-MB-231-line. We next analyzed the gene expression pattern of Pi transporters. As shown in Fig 2, MDA-MB-231 cells exhibited the highest NaPi-IIb gene expression levels when compared to the other NaPi transporters (Fig 2).
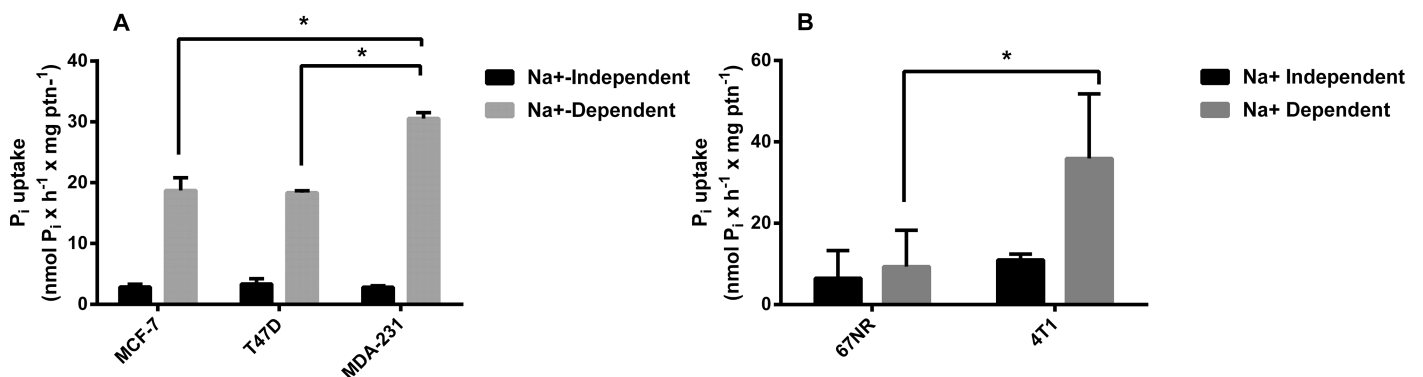
Fig 1. Comparative indices of ^{32}Pi influx in breast cancer cell lines. Intact MCF-7, T47-D or MDA-MB-231 cells (5×10^4 cells/mL = 1.45 mg protein/mL) (A) and 67NR and 4T1 (B) were incubated for 1 h at 37˚C in a reaction mixture containing 116 mM NaCl or 116 mM choline chloride, 5.5 mM Glucose, 5.4 KCl, 10 mM HEPES, 0.8 mM MgCl$_2$, 0.1 mM KH$_2$PO$_4$ and 2.5 µCi / nmol ^{32}Pi. The results are the means ± SE of at least 3 experiments, with different cell suspensions. Asterisks mark significant differences ($p \leq 0.05$) from MDA-MB-231, as determined by One-Way analysis of variance (ANOVA), using Turkey's multiple comparisons test.
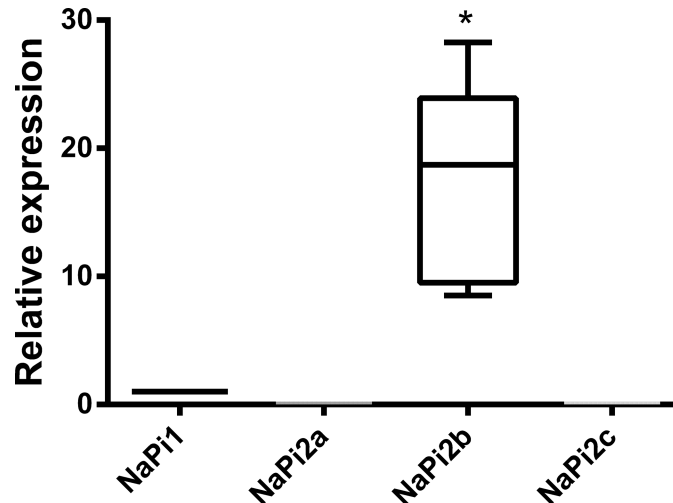
Fig 2. Gene expression analysis of Pi transporters in MDA-MB-231 cells. Total RNA was purified from MDA-MB-231 and, after treatment of RNA with DNase I, a full-length cDNA was generated from RNA. qPCR was carried. Gene expression data were normalized to an endogenous reference β-actin (ACTB). The results are the means ± SE of 7 experiments, with different cell suspensions. Asterisks mark significant differences ($p \leq 0.05$) from NaPi1, as determined by One-Way analysis of variance (ANOVA), using Turkey's multiple comparisons test.

Pi uptake and kinetic parameters

The Pi uptake in MDA-MB-231 was evaluated at different times (0 to 60 minutes) and these cells showed a linear uptake for up to 60 minutes (Fig 3A). We did not measure longer times of incorporation because it could lead to saturation. Then, all experiments were carried out at 60 minutes.

NaP$_i$-II (SLC34) is a member of the sodium-dependent P$_i$ transporter family and transports the monovalent form of P$_i$. Fig 3B shows the influence of NaCl on the Pi transport activity of MDA-MB-231 line. The kinetic parameters of this activity were: $K_{0.5} = 14.11 \pm 2.838$ mM and $V_{max} = 39.72 \pm 1.26$ nmol x h^{-1} x mg protein^{-1}.

To evaluate the affinity of the transport for P$_i$, we performed the Pi uptake in the P$_i$ concentration range of 5–500 μM (Fig 3C). The transporter followed a Michaelis-Menten kinetic and the parameter values were calculated, presenting an apparent $K_{0.5} = 84.9 \pm 10.4$ μM and a $V_{max} = 71.67 \pm 3$ nmol x h^{-1} x mg protein^{-1}.
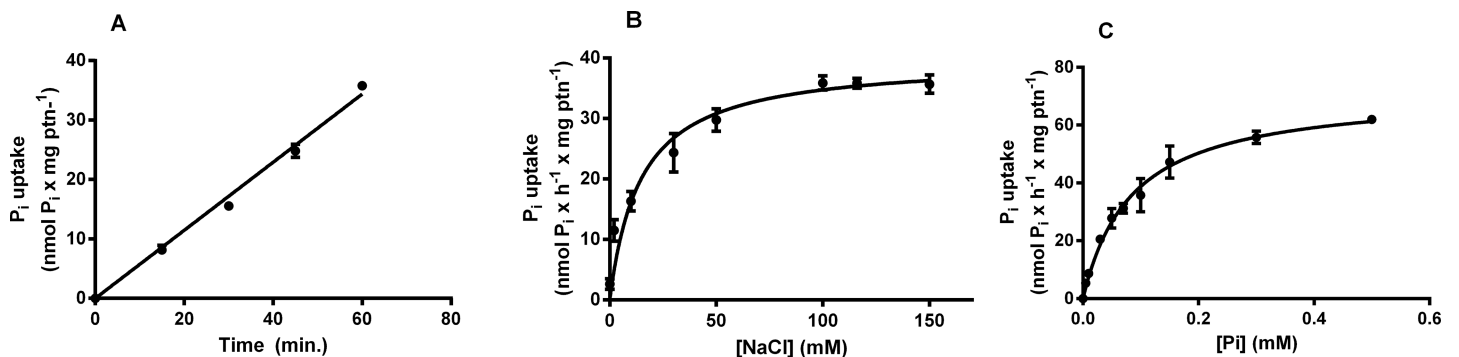
Fig 3. Time course, NaCl dependence and Pi dependence of MDA-MB-231 ^{32}Pi influx. Intact cells (5 x 10^4 cells/mL = 1.45 mg protein/mL) were incubated at 37°C in a reaction mixture containing 116 mM NaCl or 116 mM choline chloride, 5.5 mM Glucose, 5.4 mM KCl, 10 mM HEPES, 0.8 mM MgCl$_2$, 0.1 mM KH$_2$PO$_4$ and 2.5 μCi/nmol ^{32}Pi at various times (A), several NaCl concentrations (0–150 mM) (B) or various concentrations of KH$_2$PO$_4$ (0–0.5 mM) (C). The results are the means ± SE of at least 3 experiments, with different cell suspensions.
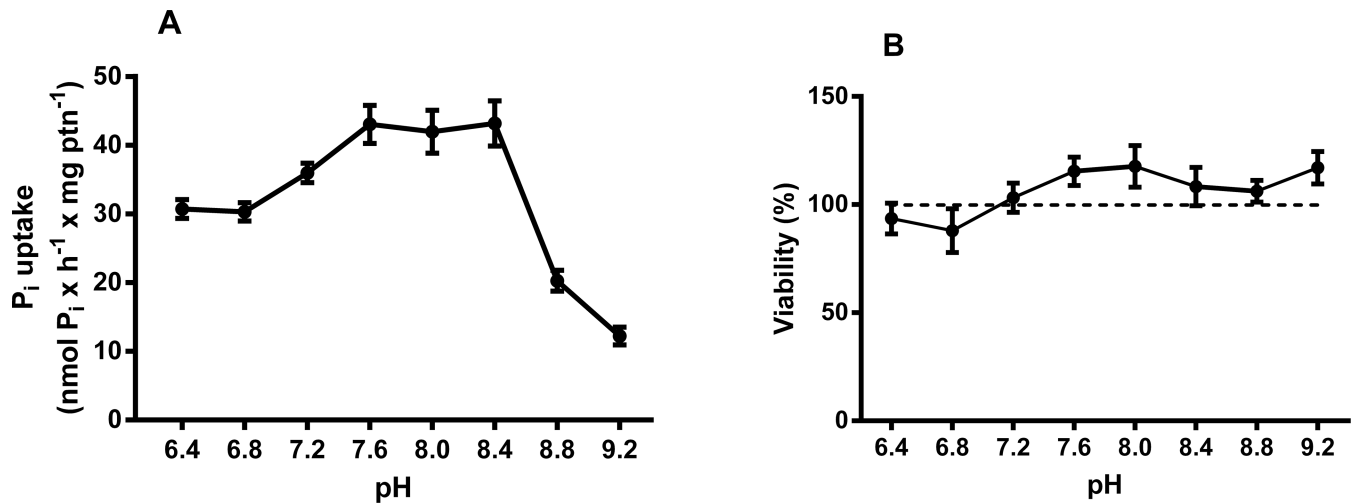
Fig 4. Effect of pH on NaCl-dependent ^{32}Pi transport in MDA-MB-231. Intact cells (5×10^4 cells/mL = 1.45 mg protein/mL) were incubated for 1 h at 37°C in a reaction mixture containing 116 mM NaCl or 116 mM choline cloride, 5.5 mM Glucose, 5.4 KCl, 0.8 mM MgCl$_2$, 0.1 mM KH$_2$PO$_4$, 2.5 µCi/nmol ^{32}Pi and 10 mM HEPES, 15 mM Tris, 15 mM MES with pH ranging from 6.4 to 9.2 (A). In these pH ranges, the cells remained viable throughout the experiment according CellTiter 96Ⓡ AQueous One Solution Cell Proliferation Assay (MTS) (B). These results are the means ± SE of at least 3 experiments, with different cell suspensions.

pH values ranging from 6.4 to 9.2 were tested, and the transport was higher at pH 7.3–7.7, as shown in Fig 4A. Fig 4B shows the cell viability during the pH experiments. Thus, all the following experiments were performed at pH 7.2, the same as the mean pH of the cell culture medium.

In order to evaluate the inhibition mechanism of Pi transport, we tested some inhibitors: bafilomycin A$_1$ (100 nM), SCH28080 (100 µM), valinomycin (100 µM), ouabain (1 mM), Furosemide (1 mM), monensin (100 µM) and PFA (5 mM) (Table 2). With the purpose of verifying the influence of H$^+$ gradient on the Pi uptake, we tested the vacuolar H$^+$ATPase inhibitor bafilomycin A$_1$ and SCH28080, a H$^+$,K$^+$-ATPase inhibitor, that were not able to inhibit the

Table 2. Effect of different agents on Pi transport of MDA-MB-231.

Condition	Activity (nmol P$_i$ x h^{-1} x mg ptn^{-1})	Viability (% of control)
CTRL	34.61 ± 4.80	100
Bafilomycin A$_1$ (100 nM)	31.57 ± 4.78	87
SCH28080 (100 µM)	34.60 ± 6.99	99
Valinomycin (100 µM)	33.70 ± 8.66	116
Ouabain (1 mM)	17.60 ± 3.67*	116
Furosemide (1 mM)	14.20 ± 3.49*	112
Monensin (100 µM)	20.70 ± 5.04*	104
PFA (5 mM)	7.65 ± 1.34*	103
Triton X 100 (1%)	-	28

Reactions were performed at 37°C in a medium (final volume: 0.5 mL) containing 116 mM NaCl or choline chloride (to calculate the Na$^+$-dependent P$_i$ transport), 5.4 mM KCl, 5.5 mM D-glucose, 0.8 mM MgCl$_2$, 50 mM Hepes, pH 7.2, 0.1 mM KH$_2$PO$_4$, 2.5 µCi/nmol ^{32}P$_i$ and 5×10^4 cells/mL (1.45 mg protein/mL) in the absence or presence of other additions, as shown in the table. The results shown are representative of at least three independent experiments. *Denotes significant differences ($p < 0.05$) after comparison with the control (no addition).
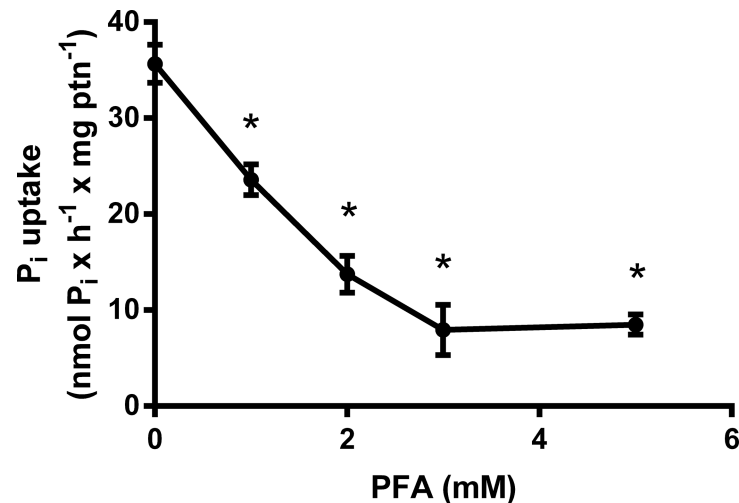
Fig 5. Effect of PFA on NaCl-dependent ^{32}Pi transport in MDA-MB-231. Intact cells (5×10^4 cells/mL = 1.45 mg protein/mL) were incubated for 1 h at 37°C in a reaction mixture containing 116 mM NaCl or 116 mM choline cloride, 5.5 mM Glucose, 5.4 KCl, 0.8 mM MgCl$_2$, 0.1 mM KH$_2$PO$_4$, 2.5 µCi/nmol ^{32}Pi and 10 mM HEPES, in the presence of increasing concentrations of PFA. In these PFA concentrations, the cells remained viable throughout the experiment. The results are the means ± SE of at least 3 experiments, with different cell suspensions. Asterisks mark significant differences (p≤ 0.05) from control, as determined by One-Way analysis of variance (ANOVA), using Turkey's multiple comparisons test.

P$_i$ transport in this cell, as well as valinomycin, a K$^+$ ionophore. Only furosemide, ouabain, monensin and PFA inhibited the Pi transport. Taken together, these data suggest the importance of Na$^+$ gradient to P$_i$ transport, possibly by the involvement of an Na$^+$,K$^+$-ATPase and/or Na$^+$-ATPase. The influence of PFA in P$_i$ transport was also verified. Increasing concentrations of this inhibitor were tested and Fig 5 shows the dose-response to PFA. These inhibitors do not affect the viability of MDA-MB-231(Table 2).
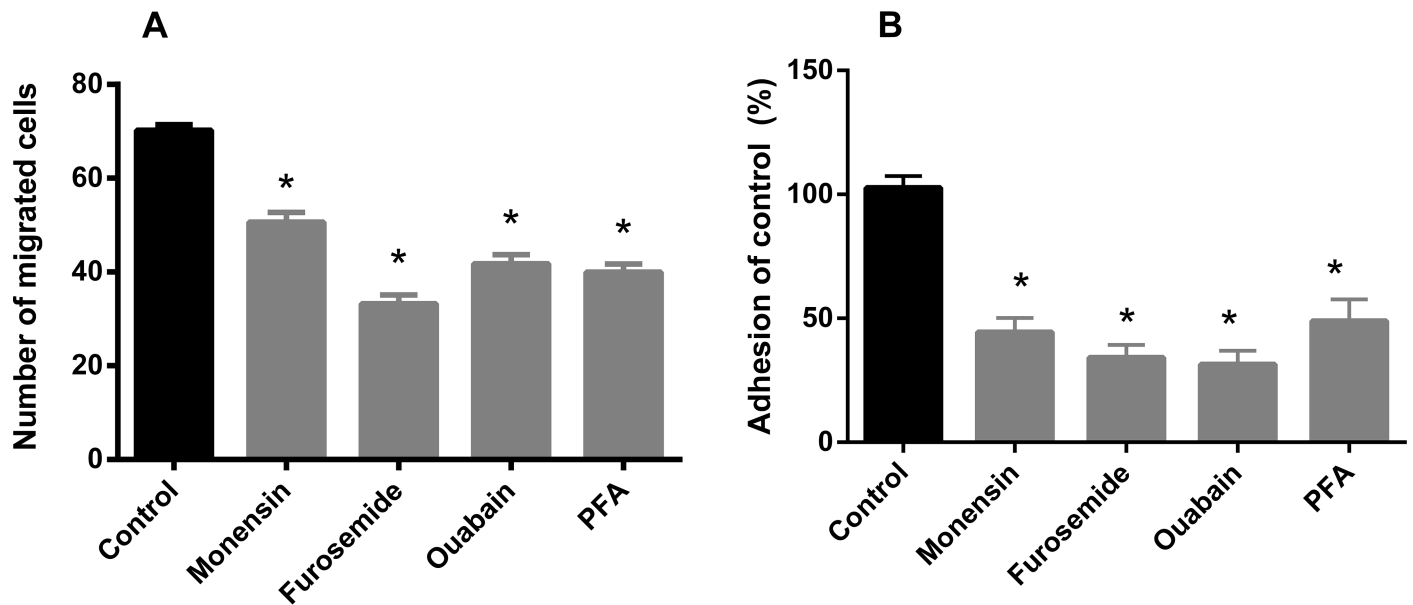
Cell migration and adhesion

In order to evaluate the possible impact of Pi transport inhibition on tumor cell properties, we further tested the effect of furosemide, ouabain, monensin and PFA on cell migration and adhesion. All inhibitors were able to inhibit the migration and adhesion of MDA-MB-231 cells (Fig 6). Pi transport inhibitors decreased cell adhesion by approximately 50%. In the case of migration, the inhibition was also significant, especially in the presence of furosemide, ouabain and PFA. These results indicate that Pi uptake is important for pro-tumoral processes such as cell motility, migration and adhesion. None of the inhibitors affected cell viability (Table 2).

Discussion

Inorganic phosphate (Pi) has been recently proposed as a key component of the "growth rate hypothesis", in which tumors exhibit high phosphorus concentration due to the requirement of a high amount of ribosomes necessary to produce proteins that support the accelerated proliferation of cancer cells [12]. Consistent with the GRH, it was reported that some tumors have higher phosphorous and RNA content than normal tissue, and that phosphorous in RNA have an important contribution to the total biomass of phosphorous in malignant rather than normal tissues [12]. More recently, it was also demonstrated that interstitial inorganic phosphate, which is elevated in tumor microenvironment, could be a new marker of tumor progression [13]. In this study, the authors propose that measurement of interstitial inorganic phosphate
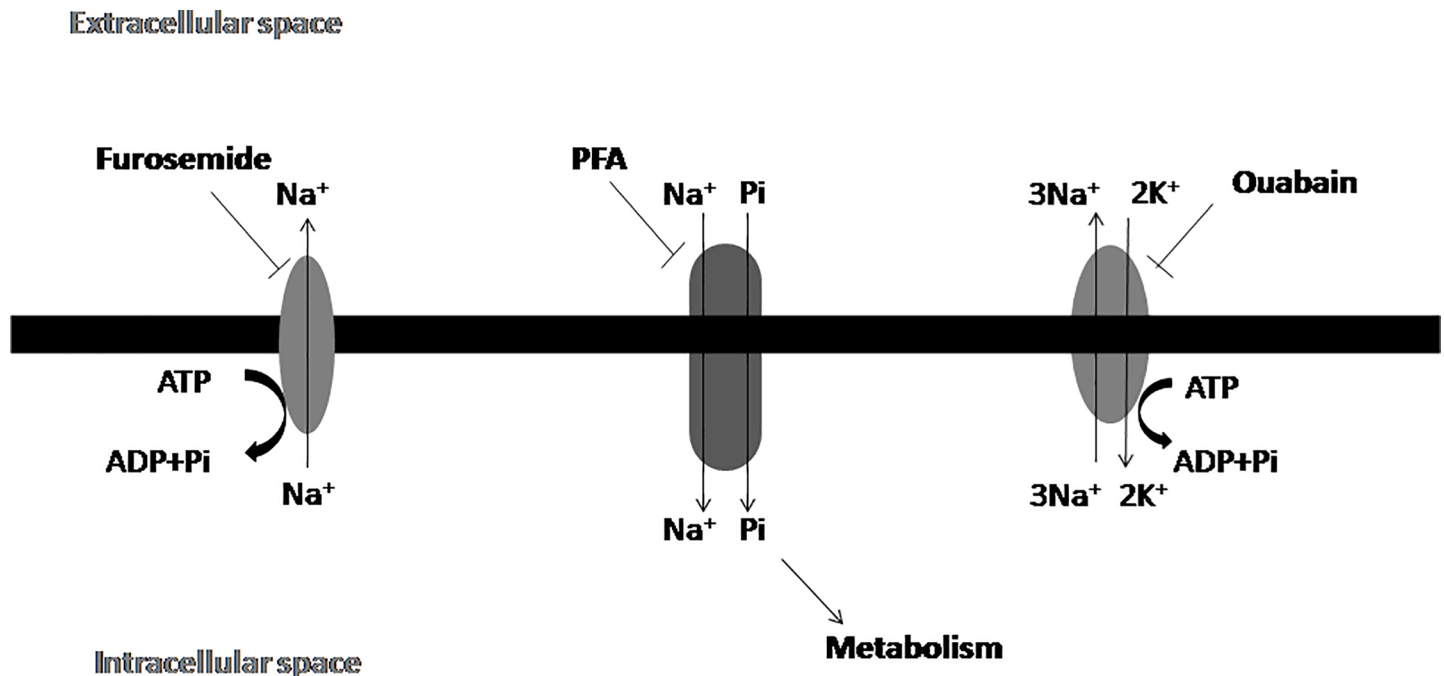
Fig 6. Effect of inhibitors on cell migration (A) and cell adhesion (B) in MDA-MB-231. Intact cells (5 x 10^5 cells/mL) were incubated for 1 h at 37˚C in a Boyden Chamber Assay™ migration (A) or in a adhesion chamber (B) in the presence or absence (control) of inhibitors indicated in the abscissa: ouabain (1 mM), furosemide (1 mM), Monensin (100 μM) and PFA (5 mM). In the presence of these inhibitors at their respective concentrations, the cells remained viable throughout the experiment. The results are the means ± SE of at least 3 experiments, with different cell suspensions. Asterisks mark significant differences ($p \leq 0.05$) from control, as determined by One-Way analysis of variance (ANOVA), using Turkey's multiple comparisons test.

https://doi.org/10.1371/journal.pone.0191270.g006

would be more sensitive and specific for tumor detection, as compared to blood Pi concentration measurements [13].

In this work we evaluated the biochemical behavior of Pi transport in an aggressive breast cancer cell line, MDA-MB-231 in an attempt to understand the importance of Pi to cancer cells. Initially, we compared the Pi transport of MCF-7, T47D and MDA-MB-231 cells. The high level of Pi transport observed in MDA-MB-231 cell line may reflect aspects of the metabolism associated to the energy demands linked to its metastatic phenotype. Conceivably, the extra Pi incorporated by MDA-MB-231 cells could be utilized as a substrate in ATP biosynthesis, thus enabling cells to sustain their typical proliferation and migration patterns. Indeed, the increased expression of Pi transporters in MDA-MB-231 cells is compatible with such a view [18,30]. Other parameters have been reported that stress the distinct metabolic identities of these cell lines. For example, MCF-7, T47D and MDA-MB-231 cells differ in lactate secretion, 2-NBDG uptake, expression of LDH and sensitivity to histone deacetylase inhibitors [31]. As a matter of fact these differences should not be surprising in view of the diverse phylogenies of MCF-7, T47D and MDA-MB-231 cell lines. Regarding the expression of Pi transporters, NaPi-IIb has been shown to be highly expressed in breast cancer [23]. We observed that the NaPi-IIb had a higher expression compared to other inorganic phosphate transporters in the MDA-MB-231 cell line (Fig 2).

Because a high expression of Pi transporters has been described in breast cancer compared to normal tissue, we have sought to identify the biochemical profile of the Pi transporter (NaPi-IIb) in kinetic terms and to correlate the transport of inorganic phosphate with the tumor processes [23]. According to Forster *et al.* [6] and Takeda [4], the Pi transporter in breast cells would be sodium dependent and with high affinity for inorganic phosphate. Partially, we correlated this high affinity of the phosphate transporter in breast cancer with the high energy requirement typical of cancer cells [30].

Extracellular space

Furosemide
Na⁺

PFA
Na⁺ Pi

3Na⁺ 2K⁺ Ouabain

ATP
ADP+Pi
Na⁺

Na⁺ Pi

ATP
ADP+Pi
3Na⁺ 2K⁺

Metabolism

Intracellular space

Fig 7. Proposed mechanism for Pi transport mechanism in MDA-MB-231 cells: Na⁺, K⁺-ATPase ouabain-sensitive in the plasma membrane and Na⁺-ATPase furosemide-sensitive plasma membrane coupled to Pi transport. Arrows indicate the direction of ion flow.

Pi is a tryptotic acid and, thus, has different physiological forms according to the pH range in which it is found [1]. Thus, when the Pi transport levels at different pH ranges were tested, we observed higher levels of transport at neutral pH than at more alkaline pH. With this result, we verified that the sodium-dependent inorganic phosphate carrier has a higher affinity for Pi in the diprotic form (H_2PO_4) found in the blood (pH 7.2).

Previous studies have demonstrated that in mammary glands NaPi-IIb was prevalently expressed as the carrier of Pi, a sodium-dependent carrier capable of transporting the Pi molecule. Furthermore, we demonstrated that the Pi transporter in tumor cells was also sodium dependent. In addition, ouabain (1 mM), furosemide (1 mM) and monensin (100 μM) were able to inhibit the transport of Pi. Furosemide inhibits the Na⁺-ATPase and ouabain inhibits the Na⁺,K⁺-ATPase. As a result the Na⁺ ion accumulates in the cytosol, leading to indirect inhibition of Pi transport. Monensin is a Na⁺ ionophore, undoing the gradient of this ion across the cytoplasmic membrane. Collectively these results suggest that the inhibitors may deregulate the intracellular sodium gradient and consequently affect sodium-dependent Pi transport (Fig 7).

Phosphonoformic acid is a competitive antagonist of the Pi transporter belonging to the NaPi-II family [32]. As expected, Pi transport into breast cancer cells in the presence of this compound was inhibited in a dose dependent manner, further evidence of the existence of the Na⁺-dependent Pi transporter on the membrane of these cells.

It was recently demonstrated in other cell types [26,33,34] that some inhibitors of Pi transport, such as FCCP, valinomycin and SCH28080, could have metabolic effects at the mitochondrial level leading to severe ATP depletion, thus indirectly affecting the active Pi uptake. Therefore, we measured the intracellular ATP content under Pi transport conditions, in the absence or presence of monensin, furosemide, ouabain and PFA, which inhibit Pi transport in MDA-MB-231 cells. However, neither inhibitor modulated cellular ATP levels (S1 Fig).

Lin *et al*. [35] identified a dose-dependence of inorganic phosphate for the cell migration of the MDA-MB-231 strain, suggesting the importance of Pi for the metastatic process. Based on this result, we sought to evaluate the importance of the Pi transporter for the metastatic process. Therefore, we used the inorganic phosphate transport inhibitors (monensin, ouabain and furosemide) and the Pi transport inhibitor (PFA) in the cell migration and adhesion assays. Interestingly, we noted a significant inhibition of cell migration, as well as cell adhesion with all inhibitors of Pi transport. PFA has been reported to inhibit the NaPi transport in osteoclast cells [36]. From these results it can be inferred that Pi directly (free Pi), or indirectly (conjugated as ATP) could be accessory to the glycolytic pathway and thus play a role in supplying energy for cellular motility and adhesion of breast cancer cells. Pi uptake appears to be related to the sodium gradient rather than to the Pi transporter itself since ouabain, furosemide and monensin decreased Pi transport, cell migration and adhesion. Therefore, the use of phosphonoformic acid clearly demonstrated that the cells were fully dependent on Pi transport for such functions.

In this study, we characterized the Pi transport in the triple-negative breast cancer cell line, MDA-MB-231. The Pi transport was found to be Na^+-dependent, had high affinity for Pi and was more active in acid pH range; it was also inhibited by classical Pi transport inhibitor, PFA. Remarkably, the inhibition of Pi transport caused significant decrease in tumor cell migration and adhesion, suggesting a prominent role for Pi transporters in tumor progression. In this context, these proteins might be regarded as potential therapeutic targets in breast cancer.

Supporting information

S1 Fig. Effect of inhibitors on ATP levels MDA-MB-231. Intact cells were incubated for 1h at 37˚C in a reaction mixture containing 116 mM NaCl or 116 mM choline chloride, 5.5 mM Glucose, 5.4 KCl, 0.8 mM MgCl2 and 10 mM HEPES, in the presence of the indicated inhibitors: monensin, furosemide, ouabain or PFA, as shown in the abscissa; 0.1 mM KH2PO4 to measure the ATP levels using an ATP bioluminescent assay Kit. The data shown are the mean activities ± SE of at least three determinations, each with different cell suspensions. Asterisks mark significant differences ($p < 0.05$) from control One-Way analysis of variance (ANOVA), using Turkey's multiple comparisons test. CTRL: control of the experiment of Pi transport in the presence of inhibitors vehicles (water, ethanol or dimethyl sulfoxide).
(TIF)

Acknowledgments

Author Contributions

Conceptualization: Thais Russo-Abrahão, Marco Antônio Lacerda-Abreu, Robson de Queiroz Monteiro, José Roberto Meyer-Fernandes.

Formal analysis: Thais Russo-Abrahão, Marco Antônio Lacerda-Abreu.

Funding acquisition: Thais Russo-Abrahão, Franklin David Rumjanek, Robson de Queiroz Monteiro, José Roberto Meyer-Fernandes.

Investigation: Thais Russo-Abrahão, Marco Antônio Lacerda-Abreu, Tainá Gomes, Daniela Cosentino-Gomes, Ayra Diandra Carvalho-de-Araújo, Mariana Figueiredo Rodrigues, Ana Carolina Leal de Oliveira.

Methodology: Thais Russo-Abrahão, Marco Antônio Lacerda-Abreu, Tainá Gomes, Daniela Cosentino-Gomes, Ayra Diandra Carvalho-de-Araújo, Mariana Figueiredo Rodrigues.

Project administration: José Roberto Meyer-Fernandes.

Resources: Thais Russo-Abrahão, Marco Antônio Lacerda-Abreu.

Supervision: Franklin David Rumjanek, Robson de Queiroz Monteiro, José Roberto Meyer-Fernandes.

Visualization: Thais Russo-Abrahão, Marco Antônio Lacerda-Abreu, Franklin David Rumjanek, Robson de Queiroz Monteiro, José Roberto Meyer-Fernandes.

Writing – original draft: Thais Russo-Abrahão, Marco Antônio Lacerda-Abreu.

Writing – review & editing: Franklin David Rumjanek, Robson de Queiroz Monteiro, José Roberto Meyer-Fernandes.

References

1. Biber J, Hernando N, Forster I. Phosphate Transporters and Their Function. Annu. Rev. Physiol. 2013; 75: 535–50. https://doi.org/10.1146/annurev-physiol-030212-183748 Review. PMID: 23398154

2. Jin H, Xu CX, Lim HT, Park SJ, Shin JY, Chung YS, et al. High Dietary Inorganic Phosphate Increases Lung Tumorigenesis and Alters Akt Signaling. Am J Respir Crit Care Med. 2009; 179(1): 59–68. https://doi.org/10.1164/rccm.200802-306OC PMID: 18849498

3. Dick CF, Santos ALA, Meyer-Fernandes JR. Inorganic phosphate uptake in unicellular eukaryotes. Biochim. Biophys. Acta. 2014; 1840(7): 2123–2127. https://doi.org/10.1016/j.bbagen.2014.03.014 PMID: 24674820

4. Takeda E, Yamamoto H, Nashiki K, Sato T, Arai H, Taketani Y. Inorganic phosphate homeostasis and the role of dietary phosphorus. J. Cell. Mol. Med. 2004; 8(2): 191–200. Review. PMID: 15256067

5. Forster IC. Phosphate transporters in renal, gastrointestinal and other tissues. Adv. in Chronic Kidney Dis. 2011; 18(2): 63–76. https://doi.org/10.1053/j.ackd.2011.01.006 PMID: 21406290

6. Forster IC, Hernando N, Biber J, Murer H. Phosphate transporters of the SLC20 and SLC34 families. Mol. Aspects Med. 2013; 34(2–3): 386–395. https://doi.org/10.1016/j.mam.2012.07.007 Review. PMID: 23506879

7. Murer H, Forster I, Biber J. The sodium phosphate cotransporter family SLC34. Pflugers Archiv—Eur. J. Physiol. 2004; 447(5): 763–767. https://doi.org/10.1007/s00424-003-1072-5 PMID: 12750889

8. Andrini O, Ghezzi C, Murer H, Forster IC. The leak mode of type II Na+-Pi cotransporters. Channels. 2008; 2(5): 346–357. PMID: 18989094

9. Vogelstein B, Papadopoulos N, Velculesco VE, Zhou S, Diaz Jr LA, Kinzler KW. Cancer genome landscapes. Science. 2013; 339 (6127): 1546–1558. https://doi.org/10.1126/science.1235122 PMID: 23539594

10. Castello A, Hentze MW, Preiss T. Metabolic enzymes enjoying new partnerships as RNA-Binding proteins. Trend Endocrinol. Metab. 2015; 26 (12): 746–57. https://doi.org/10.1016/j.tem.2015.09.012 PMID: 26520658

11. Amoedo ND. El-Bacha T, Rodrigues MF, Rumjanek FD. Cell Cycle and Energy Metabolism in Tumor Cells: Strategies for Drug Therapy. Recent Patents on Anti-Cancer Drug Discovery. 2011; 6: 15–25. PMID: 21110821

12. Elser JJ, Kyle MM, Smith MS, Nagy JD. Biological Stoichiometry in Human Cancer. PLoS ONE. 2007; 2(10): e1028. https://doi.org/10.1371/journal.pone.0001028 PMID: 17925876

13. Bobko AA, Eubank TD, Driesschaert B, Dhimitruka I, Evans J, Mohammad R, et al. Interstitial Inorganic Phosphate as a Tumor Microenvironment Marker for Tumor Progression. Sci. Rep. 2017; 7: 41233. https://doi.org/10.1038/srep41233 PMID: 28117423

14. Park JH, Lee MY, Han HJ. A potential role for caveolin-1 in estradiol-17beta-induced proliferation of mouse embryonic stem cells: involvement of Src, PI3K/Akt, and MAPKs pathways. Int J Biochem Cell Biol. 2009; 41(3): 659–65. https://doi.org/10.1016/j.biocel.2008.07.010 PMID: 18694845

15. Milani A, Geuna E, Mittica G, Valabrega G. Overcoming endocrine resistance in metastatic breast cancer: Current evidence and future directions. Help Desk: http://www.wjgnet.com/esps/helpdesk.aspx, World. J. Clin. Oncol. 2014; 10; 5(5): 990–1001. https://doi.org/10.5306/wjco.v5.i5.990 PMID: 25493235

16. Holliday DL, Speirs V. Choosing the right cell line for breast cancer research. Breast Cancer Res. 2011; 13(215): 1–7. https://doi.org/10.1186/bcr2889 PMID: 21884641

17. Ross CR, Temburnikar KW, Wilson GM, Seley-Radtke KL. Mitotic arrest of breast cancer MDA-MB-231 cells by a halogenated thieno[3,2-d]pyrimidine. Bioorg. Med. Chem. Lett. 2015; 25(8): 1715–1717. https://doi.org/10.1016/j.bmcl.2015.02.071 PMID: 25791452

18. Kwiatkowska E, Wojtala M, Gajewska A, Soszyński M, Bartosz G, Sadowska-Bartosz I. Effect of 3-bromopyruvate acid on the redox equilibrium in non-invasive MCF-7 and invasive MDA-MB-231 breast cancer cells. J. Bioenerg. Biomembr. 2016; 48(1): 23–32. https://doi.org/10.1007/s10863-015-9637-5 PMID: 26715289

19. Forster IC, Hernando N, Biber J, Murer H. Phosphate Transport Kinetics and Structure-Function Relationships of SLC34 and SLC20 Proteins. Curr. Top. in Membr. 2012; 70: 313–356. https://doi.org/10.1016/B978-0-12-394316-3.00010–7

20. Shyian M, Gryshkova V, Kostianets O, Gorshkov V, Gogolev Y, Goncharuk I, et al. Quantitative analysis of SLC34A2 expression in different types of ovarian tumors. Exp. Oncol. 2011; 33: 94–98. PMID: 21716206

21. Li Y, Chen X, Lu H. Knockdown of SLC34A2 Inhibits Hepatocellular Carcinoma Cell Proliferation and Invasion. Oncol. Res. 2016; 24: 511–519. https://doi.org/10.3727/096504016X14719078133483 PMID: 28281971

22. Jiang Z, Hao Y, Ding X, Zhang Z, Liu P, Wei X, et al. The effects and mechanisms of SLC34A2 on tumorigenicity in human non-small cell lung cancer stem cells. Tumor Biol. 2016; 37: 10383–10392. https://doi.org/10.1007/s13277-016-4928-y PMID: 26846105

23. Chen DR, Chien SY, Kuo SJ, Teng YH, Tsai HT, Kuo JH, et al. SLC34A2 as a Novel Marker for Diagnosis and Targeted Therapy of Breast Cancer. Anticancer Res. 2010; 30: 4135–4140. PMID: 21036732

24. Aslakson C.J. & Miller F.R. Selective events in the metastatic process defined by analysis of the sequential dissemination of subpopulations of a mouse mammary tumor. Cancer Res. 52, 1399–1405 (1992). PMID: 1540948

25. Bradford M M. A Rapid and Sensitive Method for the Quantitation of Microgram Quantities of Protein Utilizing the Principle of Protein-Dye Binding. Anal. Biochem. 1976; 72: 248–254. PMID: 942051

26. Russo-Abrahão T, Alves-Bezerra M, Majerowicz D, Freitas-Mesquita AL, Dick CF, Gondim KC, et al. Transport of inorganic phosphate in *Leishmania infantum* and compensatory regulation at low inorganic phosphate concentration. Biochim. Biophys. Acta. 2013; 1830(3): 2683–9. https://doi.org/10.1016/j.bbagen.2012.11.017 PMID: 23201200

27. Liu LL, Zhao H, Ma TF, Ge F, Chen CS, Zhang YP. Identification of valid reference genes for the normalization of RT-qPCR expression studies in human breast cancer cell lines treated with and without transient transfection. PLoS One. 2015; 10(1): e0117058. https://doi.org/10.1371/journal.pone.0117058 PMID: 25617865

28. Mariano-Oliveira A, De Freitas MS, Monteiro RQ, Barja-Fidalgo C. Prothrombin fragments containing kringle domains induce migration and activation of human neutrophils. Int J Biochem Cell Biol. 2008; 40 (3):517–29. https://doi.org/10.1016/j.biocel.2007.09.002 PMID: 17951099

29. Wang L, Zhou X, Zhou T, Ma D, Chen S, Zhi X, et al. Ecto-5'-nucleotidase promotes invasion, migration and adhesion of human breast cancer cells. J Cancer Res Clin Oncol. 2008; 134(3): 365–72. https://doi.org/10.1007/s00432-007-0292-z PMID: 17671792

30. Moreno-Sánchez R, Rodríguez-Enríquez S, Marín-Hernández A, Saavedra E. Energy metabolism in tumor cells. FEBS J. 2007; 10: 1393–1418. Review.

31. Rodrigues MF, Carvalho E, Pezzuto P, Rumjanek FD, Amoêdo ND. Reciprocal modulation of histone deacetylase inhibitors sodium butyrate and trichostatin A on the energy metabolism of breast cancer cells. J. Cell Biochem. 2015; 116(5): 797–808. https://doi.org/10.1002/jcb.25036 PMID: 25510910

32. Villa-Bellosta R. Sorríbas V. Different effects of arsenate and phosphonoformate on Pi transport adaptation in opossum kidney cells. Am. J. Physiol. Cell. Physiol. 2009; 297: 516–525. https://doi.org/10.1152/ajpcell.00186.2009 PMID: 19553564

33. Dick CF, Dos-Santos AL, Majerowicz D, Paes LS, Giarola NL, Gondim KC, et al. Inorganic phosphate uptake in Trypanosoma cruzi is coupled to K(+) cycling and to active Na(+) extrusion. Biochim. Biophys. Acta. 2013; 1830(8): 4265–73. https://doi.org/10.1016/j.bbagen.2013.04.034 PMID: 23643965

34. Russo-Abrahão T, Koeller CM, Steinmann ME, Silva-Rito S, Marins-Lucena T, Alves-Bezerra M, et al. H+-dependent inorganic phosphate uptake in Trypanosoma brucei is influenced by myo-inositol transporter. J Bioenerg Biomembr. 2017; 49(2): 183–194. https://doi.org/10.1007/s10863-017-9695-y PMID: 28185085

35. Lin Y, McKinnon KE, Ha SW, Beck GR Jr. Inorganic phosphate induces cancer cell mediated angiogenesis dependent on forkhead box protein C2 (FOXC2) regulated osteopontin expression. Mol. Carcinog. 2015; 54(9): 926–934. https://doi.org/10.1002/mc.22153 PMID: 24700685

36. Ito M, Haito S, Furumoto M, Uehata Y, Sakurai A, Segawa H, et al. Unique uptake and efflux systems of inorganic phosphate in osteoclast-like cells. Am J Physiol Cell Physiol. 2007; 292: C526–C534. https://doi.org/10.1152/ajpcell.00357.2006 PMID: 16971494